

# Estimation of Affine Motion from Projection Data Using a Mass Conservation Model

Mohammadreza Negahdar and Amir A. Amini, *IEEE Fellow*

**Abstract**—An approximate model for the effect of respiration is that the cross section of the thoracic area under interrogation experience time-varying magnification and displacement along two perpendicular axes – we propose to model this motion as parametric affine motion. A theoretical framework for determination of parameters of affine motion modeling the global respiratory motion based on the sinogram data in the projection domain is described. It is assumed that the spatial image considered is a density image where conservation of mass holds.

## I. INTRODUCTION

Respiratory motion results in various artifacts such as blurring and streaking in tomographic images. Tomographic projection data (sinogram data) encode not only the patient anatomy information, but also intra-scanning motion information [1]. The respiratory motion is modeled as time-varying scaling along the  $x$  and  $y$  direction. A simplified cross section of a patient lying supine in a CT scanner is shown in figure 1, where the patient's back is resting on the scan table at  $(x_p, y_p)$ . We assume that respiration causes a time-varying magnification, denoted  $m_x$  and  $m_y$ , about the  $x$  and  $y$  axes, respectively [2], expressible as an affine motion [3].

A fundamental problem in both image sequence processing and computer vision is estimation of the image motion in a temporal sequence of frames; a great deal of effort has been devoted to this problem in the past [3-7]. Time-varying image sequences are typically modeled as a space-time evolving function  $f(x, y, t)$  where  $x$  and  $y$  represent the spatial coordinates in the image plane and  $t$  is the time variable. Written with respect to a reference frame chosen at time  $t = 0$ , we then have the model

$$f(x, y, t) = f(x - v_1(x, y)t, y - v_2(x, y)t, 0) \quad (1)$$

where  $v_1(x, y)$  and  $v_2(x, y)$  denote the components of the velocity (motion) vector field  $\vec{v}$  and where it is assumed that higher order components of the motion field such as acceleration and jerk are identical to zero. In this paper, we are concerned with estimating the class of vector fields  $\vec{v}$  parameterizable by an affine model. Therefore, the vector

fields of interest are characterized by

$$\vec{v} = \vec{v}_0 + M \begin{bmatrix} x \\ y \end{bmatrix}, \quad (2)$$

where

$$\vec{v}_0 = \begin{bmatrix} v_{0x} \\ v_{0y} \end{bmatrix}, \quad (3)$$

is a constant vector representing global translational motion, and

$$M = \begin{bmatrix} a & b \\ c & d \end{bmatrix}, \quad (4)$$

captures dynamics of body motions as manifested in the image plane.

While there are many methods for estimating affine vector fields, we base our analysis on the image projections which provide an effective and efficient way of describing image contents and estimate particular kinds of motion. For instance, the problem of 2D translational motion estimation can be reduced to two 1D translational motion estimation by using projections. This reduction may bring both algorithmic and computational simplifications. However, this requires the availability of a proper mapping model which describes how to map a problem into a number of simple problems.

The aim of this paper is to exploit the gradient-based methods in the projection domain via Radon transform to yield fast, and accurate estimation of the motion parameters. The Radon Transform of an image is defined as line integrals across the image[8]. The shift property of the Radon transform states that pure translational motion in an image results in translation of the projections along the direction of projection [8, 9]. In particular, it can be shown that affine motion in the image leads to affine motion in the projections as well [9-11]. These properties were modeled as a motion mapping model in [10] and has been used in the

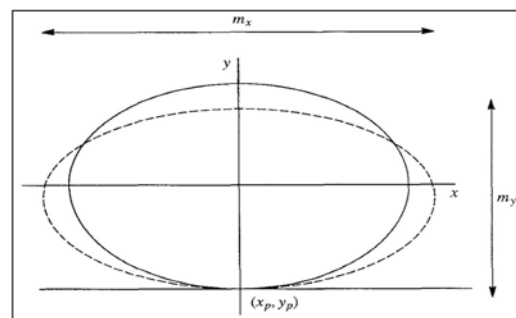


Figure 1: Outline of cross section of chest during respiration. Solid and dash lines represent different samples in the respiratory cycle [2].

Manuscript received April 7, 2011.

Mohammadreza Negahdar is a PhD Candidate with the Medical Imaging Lab (MIL), Electrical and Computer Engineering Department, University of Louisville, KY 40292 USA. (phone: 502-553-9800, e-mail: m0nega01@louisville.edu).

Amir Amini is Professor and Endowed chair in Bioimaging, Director of MIL, Electrical and Computer Engineering Department, University of Louisville, KY 40292 USA. (e-mail: Amir.Amini@louisville.edu).

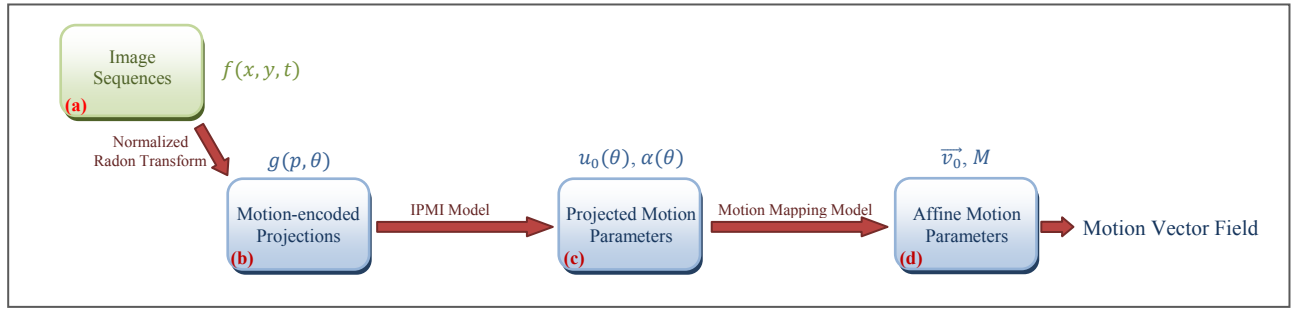


Figure 2: Image motion estimation in the Radon transform domain.

past to estimate motion from projections [1, 10-12]. However, the proposed model in [10] is based on differential gradient-based models and as will be shown though effective for simple forms of affine motion, can result in large errors when the motion is non-rigid and includes shearing or linear divergence.

The proposed algorithm in this paper is able to cope with the aforementioned difficulty in estimating affine motion. Nonetheless, as a limitation of all affine motion estimation techniques including the one presented here (the so-called motion mapping models), only 5 of the 6 affine parameters can be estimated. Therefore, the work presented here is an important step forward in estimating parametric affine motion from image projections. In particular, this model is valid and more accurate than previously proposed techniques when dealing with density images where the physical principle of mass conservation holds. A good example of this scenario holds in CT images of lung as modeled in figure 1.

The paper is organized as follows. First, a brief overview of the motion in the projection domain is given. Subsequently, the affine motion estimation algorithm based on projections as well as our proposed algorithm in estimation of the projected and affine motion parameters is introduced and derived. Next, experimental results and comparison with previous methods are presented. Finally, the main conclusions and some ideas for further work are presented.

## II. METHOD

In the proposed algorithm in this paper (figure 2), a set of projection signals of two consecutive images (block a) is estimated via the normalized Radon transform (block b), Subsequently, 1D affine motion between each pair of corresponding projection signals is estimated (block c). Please see section A for details of these steps. Finally, 2D image affine motion is derived from the set of estimated 1D motion parameters, using a motion mapping model (block d). Please see section B for a description of this part.

### A. Motion in the Projection Domain

The Radon transform of an image  $f(x, y)$  is defined as [8]

$$g(p, \theta) = \mathcal{R}_\theta[f(x, y)] = \iint f(x, y) \delta(p - x \cos \theta - y \sin \theta) dx dy \quad (5)$$

The normalized Radon transform defined in [11] is

$$\tilde{g}(p, \theta) = \tilde{\mathcal{R}}_\theta[f(x, y)] = \frac{\iint f(x, y) \delta(p - x \cos \theta - y \sin \theta) dx dy}{\iint \delta(p - x \cos \theta - y \sin \theta) dx dy} \quad (6)$$

This definition normalizes the radon transform with respect to ray length and in projection domain produces a 1D constant projection of a constant image irrespective of size. Technically speaking, this definition gives more accurate results when computing derivatives from projection data, however; in theory, derivations are identical with both approaches.

One of the most fundamental and useful properties of the Radon transform is that shifting of the image results in a shifted projection [8, 10]. This relates translational motion in the image domain to simple displacement in the projection domain.

$$\mathcal{R}_\theta[f(x - v_{0x}, y - v_{0y})] = g(p - \vec{v}_0^T \vec{\omega}, \theta) = g(p - u_0(\theta), \theta) \quad (7)$$

where  $\vec{\omega} = [\cos \theta \ \sin \theta]^T$  is a unit directional vector. The question of how general motion in image sequences behave under tomographic projection was addressed in [10] where it was shown that under certain smoothness conditions on the image and the vector field  $\vec{v}$ , for sufficiently small  $\Delta t$ , there exists a unique function  $u(p, \theta)$  such that

$$\mathcal{R}_\theta[f(x - v_1 \Delta t, y - v_2 \Delta t)] = g(p - u(p, \theta) \Delta t, \theta) \quad (8)$$

where

$$u(p, \theta) \frac{\partial g(p, \theta)}{\partial p} = \mathcal{R}_\theta[\vec{v}^T \nabla f] \quad (9)$$

As in [9, 10], we refer to equation (9) as the Projected Motion Identity (PMI). This relationship states that the projection of a dynamic image sequence evolves in a qualitatively similar fashion as the original image sequence. That is, the projection function  $g(p, \theta)$  evolves a transformation or warping of the domain coordinates  $p$  by the function  $u(p, \theta)$ .

A straightforward corollary of the above result is that

under the same assumptions, we have

$$\frac{dg}{dt} = \mathcal{R}_\theta \left[ \frac{df}{dt} \right] \quad (10)$$

That is, locally, the projection of the total derivative of  $f$  is the total derivative of the projection of  $f$ . An immediate consequence shown in reference [8] is that if the optical flow brightness constraint  $\frac{df}{dt} = 0$  is assumed to hold in the image domain, then equation (10) implies that this constraint also holds in the projection domain:  $\frac{dg}{dt} = 0$ , with motion in this domain given by (9).

By invoking the directional derivative property<sup>1</sup> [8, 10], we can express PMI as follows:

$$u(p, \theta, t) \mathcal{R}_\theta[\omega^T \nabla f] = \mathcal{R}_\theta[\vec{v}^T \nabla f] \quad (11)$$

However, other forms of the PMI are also possible. Namely, Fitzpatrick [13] considered  $f$  and  $v$  to both be  $C^1$  continuous, where,  $f$  is to represent the density of some conserved quantity. In that case,

$$\frac{df}{dt} + \text{div}(fv) = 0 \quad (12)$$

Taking the Radon transform of both sides of (12), and applying the directional derivative property we have

$$\begin{aligned} & \frac{\partial g}{\partial t} + \mathcal{R}_\theta \left[ \frac{\partial(fv_1)}{\partial x} \right] + \mathcal{R}_\theta \left[ \frac{\partial(fv_2)}{\partial y} \right] \\ &= \frac{\partial g}{\partial t} + \omega_1 \frac{\partial}{\partial p} \mathcal{R}_\theta[fv_1] + \omega_2 \frac{\partial}{\partial p} \mathcal{R}_\theta[fv_2] \\ &= \frac{\partial g}{\partial t} + \frac{\partial}{\partial p} \mathcal{R}_\theta[fv^T \omega] = 0 \end{aligned} \quad (13)$$

Now if we define

$$u_c(p, \theta, t)g(p, \theta, t) = \mathcal{R}_\theta[fv^T \omega] \quad (14)$$

We obtain the continuity equation for  $g$ :

$$\frac{\partial g}{\partial t} + \frac{\partial(u_c g)}{\partial p} = 0 \quad (15)$$

The identity (14) is the PMI implied by the mass conservation principle which can be referred to as the Integral PMI (IPMI), while referring to (9) as the differential PMI (DPMI). Similar to the DPMI, the IPMI also implies a description of  $u$  as the ratio of two projection:

$$u_c(p, \theta, t) \mathcal{R}_\theta[f] = \mathcal{R}_\theta[fv^T \omega] \quad (16)$$

That is,  $u_c$  is the ratio of the projection of the flux ( $fv$ ) in the direction of  $\omega$ , to the projection of  $f$  itself in the same direction.

We now present a method for estimating the projected motion parameters from projections at a fixed angle  $\theta$  over time based on the optical flow method. By expanding (12) in a Taylor series truncated to the first order and applying the directional derivative property we obtain

$$\begin{aligned} \mathcal{R}_\theta[\nabla f \cdot v + f \nabla \cdot v] &= -\frac{\partial g}{\partial t} \\ \frac{\partial g}{\partial p} u(p, \theta) + g \frac{\partial u(p, \theta)}{\partial p} &= -\frac{\partial g}{\partial t} \\ g_p u + g u_p &= -g_t \end{aligned} \quad (17)$$

Where  $g_p$  and  $u_p$  denotes the partial derivatives of  $g$  and  $u$  with respect to the location variable  $p$ , respectively, and  $g_t = g(p, \theta, 1) - g(p, \theta, 0)$ .

### B. Effect of the 2D Affine Motion in the Projection Domain

Any motion field can be locally approximated (to first order) by affine motion as considered in equation (2) [3, 10]. Affine motion can be decomposed into rotational, divergent, and shearing components. That is, the matrix  $M$  can be written as follows:

$$M = \frac{a+d}{2} \begin{bmatrix} 1 & 0 \\ 0 & 1 \end{bmatrix} + \frac{c-b}{2} \begin{bmatrix} 0 & -1 \\ 1 & 0 \end{bmatrix} + \frac{a-d}{2} \begin{bmatrix} 1 & 0 \\ 0 & -1 \end{bmatrix} + \frac{b+c}{2} \begin{bmatrix} 0 & 1 \\ 1 & 0 \end{bmatrix} \quad (18)$$

where the first term of the above sum corresponds to linear divergent motion represented by  $\begin{bmatrix} x \\ y \end{bmatrix}$ ; the second term corresponds to rotational motion represented by  $\begin{bmatrix} y \\ -x \end{bmatrix}$ ; and the final two terms correspond to shearing motions represented by  $\begin{bmatrix} x \\ -y \end{bmatrix}$  and  $\begin{bmatrix} y \\ x \end{bmatrix}$ , respectively [9].

To see how affine transformation behaves in the projection domain, let us consider warping an image by such a transformation. By computing the derivative of both sides of the IPMI with respect to  $p$

$$\begin{aligned} & \frac{\partial}{\partial p} (u_c g) = \frac{\partial}{\partial p} (\mathcal{R}_\theta[fv^T \omega]) \\ &= \frac{\partial}{\partial p} (\mathcal{R}_\theta[f((ax + by)\omega_1 + (cx + dy)\omega_2)] + \mathcal{R}_\theta[fv_0^T \omega]) \\ &= \frac{\partial}{\partial p} (\mathcal{R}_\theta[x(a\omega_1 + c\omega_2)f + y(b\omega_1 + d\omega_2)f]) + \frac{\partial}{\partial p} (gv_0^T \omega) \\ &= \frac{-\partial}{\partial \omega_1} \mathcal{R}_\theta[(a\omega_1 + c\omega_2)f] - \frac{\partial}{\partial \omega_2} \mathcal{R}_\theta[(b\omega_1 + d\omega_2)f] + \frac{\partial}{\partial p} (gv_0^T \omega) \\ &= -\left( ag + (a\omega_1 + c\omega_2) \frac{\partial g}{\partial \omega_1} \right) - \left( dg + (b\omega_1 + d\omega_2) \frac{\partial g}{\partial \omega_2} \right) + \frac{\partial}{\partial p} (gv_0^T \omega) \\ &= -\left( \text{tr}(M)g + \omega^T M \begin{bmatrix} \frac{\partial g}{\partial \omega_1} \\ \frac{\partial g}{\partial \omega_2} \end{bmatrix} \right) + \frac{\partial}{\partial p} (gv_0^T \omega) \end{aligned}$$

Therefore,

$$(u_c - v_0^T \omega) \frac{\partial g}{\partial p} + \text{tr}(M)g + \omega^T M \begin{bmatrix} \frac{\partial g}{\partial \omega_1} \\ \frac{\partial g}{\partial \omega_2} \end{bmatrix} = 0 \quad (19)$$

$$(u_c - v_0^T \omega) \frac{\partial g}{\partial p} + \text{div}(gM^T \omega)|_{|w|=1} = 0 \quad (20)$$

By using some properties of the Radon transform, as well as some approximations, the projection motion model in (20)

<sup>1</sup> Transform of Derivative: Let  $L(\frac{\partial}{\partial x}, \frac{\partial}{\partial y})$  denote a linear differential operator. We have:  $\mathcal{R}_\theta[Lf] = L(\omega_1 \frac{\partial}{\partial p}, \omega_2 \frac{\partial}{\partial p})g(p, \omega)$ .

can be written as [10]

$$u(p, \theta) \approx v_0^T \omega + (\omega^T M \omega) p = u_0(\theta) + \alpha(\theta) p \quad (21)$$

This states that the projected motion  $u(p, \theta)$  is also an affine function of the radial parameter  $p$ , and is parameterized by  $u_0(\theta)$  and  $\alpha(\theta)$ .

### III. RESULTS

In this part we explicitly work out analytical expressions for  $u(p, \theta, t)$  for two different image sequences and vector fields. These examples are exactly those which were presented in [9] yielding an image to compare the performance of the approach in [9-11] which was based on DPML with our proposed method which is based on IPML.

#### A. Linear Divergence in a Symmetric Magnification

Let  $f(x, y, t) = \exp(-(x - v_1 t)^2 - (y - v_2 t)^2)$ , and  $v(x, y) = [x, y]^T$ , as shown in figure 2. Computing the gradient of  $f$ :

$$\nabla f = -2(1-t)^2 \exp(-(1-t)^2(x^2 + y^2)) \begin{bmatrix} x \\ y \end{bmatrix} \quad (22)$$

$$\begin{aligned} \mathcal{R}_\theta[\vec{v}^T \nabla f] &= \mathcal{R}_\theta[-2(x^2 + y^2)(1-t)^2 \exp(-(1-t)^2(x^2 + y^2))] \\ &= \frac{-\sqrt{\pi} \exp(-p^2(1-t)^2)}{|1-t|} (2p^2(1-t)^2 + 1) = -g_t \end{aligned} \quad (23)$$

$$\frac{\partial g(p, \theta, t)}{\partial p} = \frac{-\sqrt{\pi} \exp(-p^2(1-t)^2)}{|1-t|} (2p(1-t)^2) = g_p \quad (24)$$

$$\mathcal{R}_\theta[f \nabla \cdot \vec{v}] = \frac{\sqrt{\pi} \exp(-p^2(1-t)^2)}{|1-t|} = g_{u_p} \quad (25)$$

$$u_c = \frac{2p^2(1-t)^2 + 1 - 1}{2p(1-t)^2} = p \quad (26)$$

By comparing with (21)

$$M = \begin{pmatrix} 1 & 0 \\ 0 & 1 \end{pmatrix} \quad (27)$$

While the computed projected motion with the proposed algorithm in [9-11] get

$$u = p + \frac{1}{2p(1-t)^2} \quad (28)$$

Clearly, the proposed algorithm gives more exact answer.

#### B. Rotational Motion

Let  $f(x, y, t) = [(x - v_1 t) + (y - v_2 t)] \exp(-(x - v_1 t)^2 - (y - v_2 t)^2)$  which is not rotationally symmetric, and  $v(x, y) = [-y, x]^T$ . Since  $f \nabla \cdot \vec{v} = 0$ , the proposed method simplifies to the previous method in [9-11];

$$u(p, \theta, t) = \frac{p[(t+1) \cos \theta + (t-1) \sin \theta]}{(1-2p^2(1+t^2))[(t+1) \sin \theta - (t-1) \cos \theta]} \quad (29)$$

### IV. CONCLUSIONS

Given the decomposition in (18), the linearity property implied by PMI shows that the projection of any affine motion has a natural decomposition into translational, rotational, divergent, and shearing components.

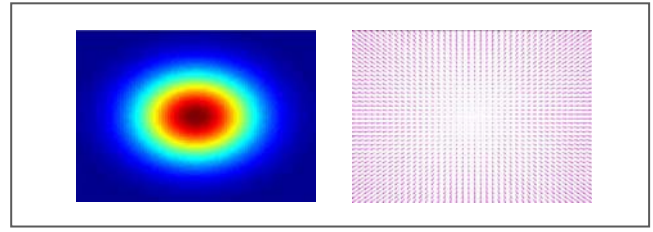


Figure 3: The color coded image in Example 1 and its motion field.

Obviously, the proposed model is only valid when the continuity equation holds; that is, when it can be assumed that the image intensities are related to mass densities and that therefore mass conservation holds. In that case, affine motion which consists of linear divergence and/or shearing (example 1) would be estimated more accurately by application of our proposed method. Otherwise (example 2), the proposed method in this paper simplifies to the method previously proposed in [9-11].

### REFERENCES

- [1] W. Lu, and T. R. Mackie, "Tomographic motion detection and correction directly in sinogram space," *Physics in Medicine and Biology*, vol. 47, no. 8, pp. 1267-1284, 2002.
- [2] C. R. Crawford, K. F. King, C. J. Ritchie *et al.*, "Respiratory compensation in projection imaging using a magnification and displacement model," *IEEE Transactions on Medical Imaging*, vol. 15, no. 3, pp. 327-332, 1996.
- [3] C. Stiller, and J. Konrad, "Estimating motion in image sequences," *IEEE Signal Processing Magazine*, vol. 16, no. 4, pp. 70-91, 1999.
- [4] L. G. Brown, "A survey of image registration techniques," *ACM Comput. Surv.*, vol. 24, no. 4, pp. 325-376, 1992.
- [5] J. L. Barron, D. J. Fleet, and S. S. Beauchemin, "Performance of optical flow techniques," *International Journal of Computer Vision (IJCV)*, vol. 12, no. 1, pp. 43-77, 1994.
- [6] S. Alliney, and C. Morandi, "Digital Image Registration Using Projections," *IEEE Trans. on Pattern Analysis and Machine Intelligence*, vol. PAMI-8, no. 2, pp. 222-233, 1986.
- [7] J. Weickert, A. Bruhn, and C. Schnorr, "Lucas/Kanade meets Horn/Schunck: combining local and global optic flow methods," *International Journal of Computer Vision*, vol. 61, no. 3, pp. 211-231, 2005.
- [8] S. R. Deans, *The Radon Transform and Some of its Applications*, Malabar, FL: Krieger 1993.
- [9] P. Milanfar, "Motion from projections," in SRI Int. Tech. Rep., 1997.
- [10] P. Milanfar, "A model of the effect of image motion in the Radon transform domain," *IEEE Trans. on Image Processing*, vol. 8, no. 9, pp. 1276-1281, 1999.
- [11] D. Robinson, and P. Milanfar, "Fast local and global projection-based methods for affine motion estimation," *J. Math. Imaging and Vision*, vol. 18, no. 1, pp. 35-54, 2003.
- [12] V. J. Traver, and F. Pla, "Motion Analysis with the Radon Transform on Log-Polar Images," *J. Math. Imaging and Vision*, vol. 30, no. 2, pp. 147-165, 2008.
- [13] J. M. Fitzpatrick, "The existence of geometrical density-image transformations corresponding to object motion," *Comput. Vis., Graphics and Image Process.*, vol. 44, pp. 155-174, 1988.